Detailed Investigation of PC Cable-stayed Bridge Damaged in the 1999 Taiwan Earthquake

Kenji KOSA[1] and Kenji TASAKI [2]

ABSTRACT

Among the bridges damaged in the 1999 Chi-Chi earthquake in Taiwan, the Ji-Ji-Da Bridge (cable-stayed) suffered problematic damage which is unacceptable in terms of seismic design of this type of bridge. For example, plastic hinges were produced not only at the pier bottom but also in the main pylon and the main girder, and one diagonal cable pulled out from the anchorage section. The damage mechanism of this bridge was analyzed using a frame model, with the incorporation of field measurement results and detailed drawings obtained from bridge administrators in Taiwan. It was found that that the cause of cable pullout was the insufficient anchoring strength.

1. INTRODUCTION

Tremendous damage was caused in the central region of Taiwan in the Chi-Chi Earthquake that occurred in Sept. 1999 with a magnitude of M=7.3. Many bridges fell or suffered a crucial damage in the area along the Chelungph Fault that runs north to south near the hypocenter shown in Fig. 1. Among the damaged bridges, the cable-stayed Ji-Ji-Da Bridge which was under construction at the time suffered a problematic damage that needs discussion in terms of seismic design. For example, damage occurred not only to the bottom of the pier but also to the main pylon and the main girder, in addition to the pullout of a diagonal cable from the anchorage section. In view of the importance of the damage, various investigations, such as linear dynamic analysis and strength check, have been carried out nationally and internationally, including ours [1)-3)]. Our previous investigation was not fully successful in identifying the cause of damage of this bridge, partly because the analysis was performed based on limited information.

To pursue the problem, the authors once again visited the damage site in Taiwan in November 2002 to conduct a field survey and to see the progress of retrofit. At that time, we had a chance to talk with bridge administrators in Taiwan and could get detailed drawings of the bridge. Using the information thus obtained and the results of micro-vibration measurement taken at the bridge site, a detailed investigation was conducted on the damage mechanism of this bridge. This paper presents the results of this investigation.

---

1) Professor of Civil Engineering, Kyushu Institute of Technology, Kitakyushu, Japan
2) Senior Engineer, Structural Engineering Division, Nippon Engineering Consultants Co., Ltd. (Currently in the doctoral program at Kyushu Institute of Technology)

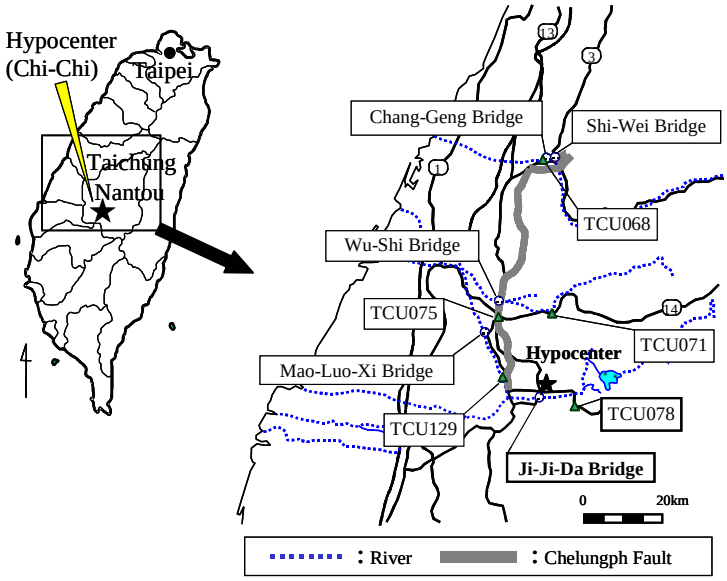

Fig. 1 Bridges surveyed and measuring locations of strong motion

2. STRUCTURE OF THE BRIDGE AND OUTLINE OF DAMAGE

The Ji-Ji-Da Bridge is a PC cable-stayed bridge with two spans which is located at about 3 km away from the hypocenter at Chi-Chi. At the time of the earthquake, this bridge was under construction and four panels of precast members on one side at the connection area of the main pylon and the main girder were not yet built, as shown in Fig. 2.

The main girder of this bridge consists of arc-curved one box girder with two cells. The girder height is 2.75 m, the girder width is 24.0 m and the span length is @120 x 2 = 240 m. The main pylon is an RC column, 58 m in height, having a deformed diamond shaped cross section with a hollow, measuring 3.0 m x 4.0-6.0m, as shown in Figs. 3 and 4. The cables are arranged in two rows. In one row, 17 cables are arranged on each side of the main pylon. The pier below the main pylon is an oval-shaped RC column measuring 6.0 x 6.3 m, as seen in Fig. 5. The Foundation below the main pylon is the cast-in-place pile type (ϕ1500). The concrete strength (σck) is 34.3 N/mm^2 for all of the main girder, the main pylon, and the pier.

The damage was widespread extending over the main girder, the main pylon, the pier, as well as the cable, as shown in Fig. 2. For example, the cover concrete fell from the faces of the perpendicular direction at the bottom of the main pylon, and the ends of the main girder detached from each adjoining girder and swayed to the perpendicular direction. Also, the cover concrete was separated and the main reinforcement buckled in the main girder on the south side at the rigid connection section with the main pylon. From these damages, it is considered that a large seismic force acted in both the axial direction and the perpendicular direction of the bridge.

As to the cables, one cable on the south side, the 11th from the top, was pulled out from the anchorage section of the main pylon. Many sockets were also pulled out from the anchorage section. This means that large tension was caused to the diagonal cables during the earthquake. On the other hand, according to our first field measurement immediately after the earthquake, the span length before the earthquake, 120 m, did not changed virtually after the earthquake.

In view of the fact that (a) a fault was not found in the vicinity of the bridge and (b) the seismic waveform obtained at TCU078 (to be explained later) did not show any waveform like a directivity pulse even though its location is close to the Chelungph Fault, it is considered that the damage occurred to this bridge was primarily caused by the seismic motion during the earthquake.

As to the progress of retrofit as of November 2002, Ji-Ji-Da Bridge was already open for service, but the pullout cable was still left as it was and a bent support was still in place. However, the bottom of the main pylon had been repaired with concrete jacketing and the bottom of the pier with steel jacketing.

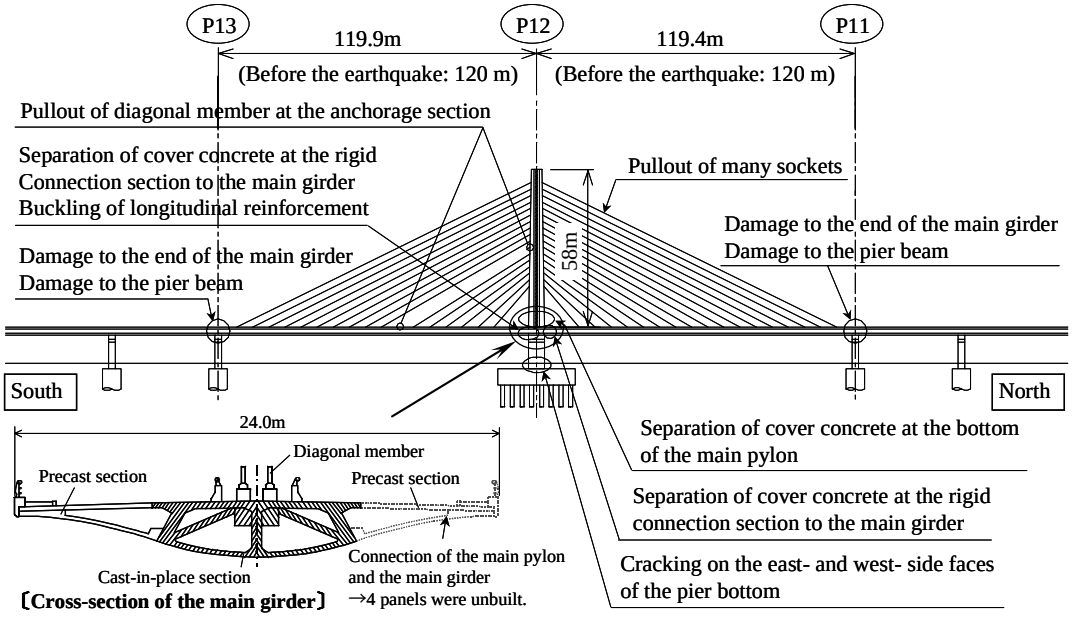

Fig. 2 Damage to the Ji-Ji-Da Bridge and measurement results

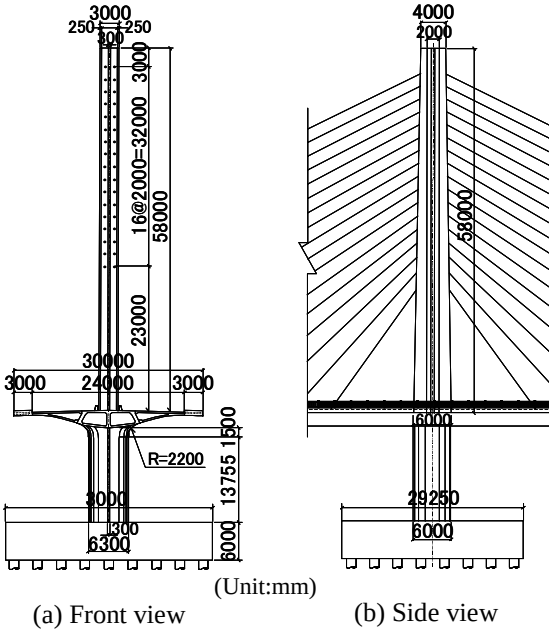

Fig. 3 Structure of the main pylon

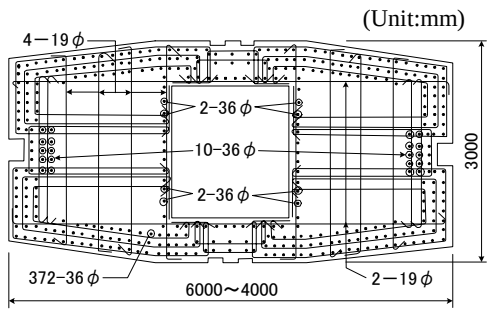

Fig. 4 Cross section of the main pylon

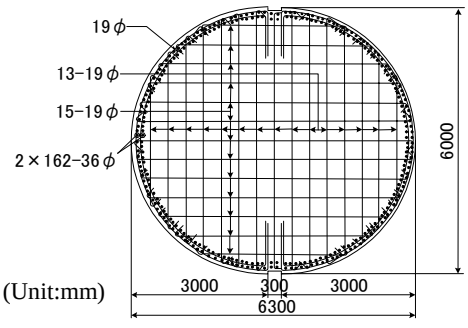

Fig. 5 Cross section of the pier at the main pylon

3. SEISMIC RESPONSE ANALYSIS

3.1 Analysis Model

The main span (@120 x 2 = 240 m) of the Ji-Ji-Da Bridge shown in Fig. 2 was modeled as the 3D frame model, as shown in Fig. 6, and a nonlinear time history response analysis was performed using this model. The sectional constants of the main girder, the main pylon, and the pier shown in Table 1 were determined based on the detailed drawings of the reinforcement arrangement. The bending moment-curvature relationships (M-ϕ)of the main pylon and the pier were calculated by considering the level of the axial force when the dead load is working. In the frame model, the main girder was modeled by the elastic beam elements, the main pylon and the pier by the elasto-plastic beam elements, and the diagonal cables by the linear truss elements having the stiffness only in the axial direction. As to the rigid connection section of the main pylon and the main girder, rigid elements were placed as shown in Fig. 6. The mass of the cables was divided into two and each was added to each joint on the main pylon and the main girder at the end of the elements. As to the boundary conditions, the only conditions fixed were the bearing conditions in the vertical and perpendicular directions of the piers (Pier 11 and Pier 13).

(1) Modeling of the main girder

As said earlier, four panels of precast members on one side of the main girder were unbuilt at the time of the earthquake. In the analysis model, this effect was taken into account in the flexural rigidity of the main girder. As shown in Fig. 7, the 6.0-m section which is equal to the width in the axial direction at the bottom of the pylon was modeled as the rigid members, and the two 0.68-m sections were modeled as the elastic beam elements in consideration of the incompleteness of the cross section.

Table 1 Constants of the cross-section

Cross section	Geometrical moment of inertia (m^4)			Yield bending moment (MN・m)		Yield curvature (1/m)		Sectional area (m^2)
	Ix	Iy	Iz	Myox	Myoy	ϕyox	ϕyoy	A
Main girder (built section)	-	15.10	1579.67	-	-	-	-	15.732
Main girder (unbuilt section)	-	14.71	450.97	-	-	-	-	12.571
Top of the main pylon	9.51	11.26	-	89.50	133.43	7.942E-4	4.077E-4	8.905
Bottom of the main pylon	13.13	53.74	-	180.31	324.16	9.319E-4	4.479E-4	14.120
Pier	86.26	79.54	-	426.72	415.12	4.546E-4	4.771E-4	30.074
Average of the cables	-	-	-	-	-	-	-	0.0092
[Definitions of the structural axes] X axis: axial direction, Y axis: perpendicular direction, Z axis: vertical direction								

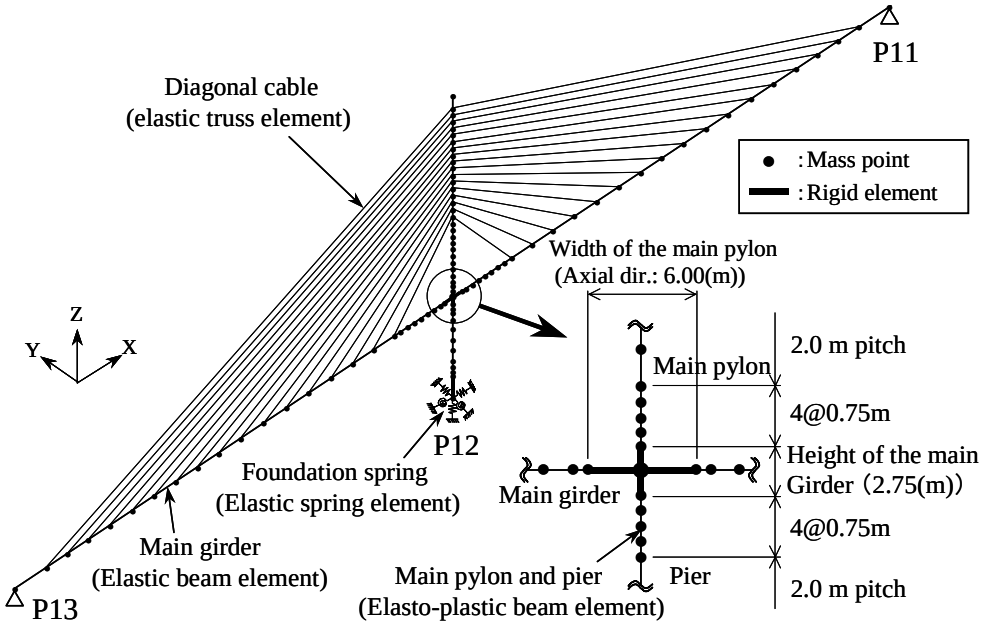

Fig. 6 Frame model for analysis

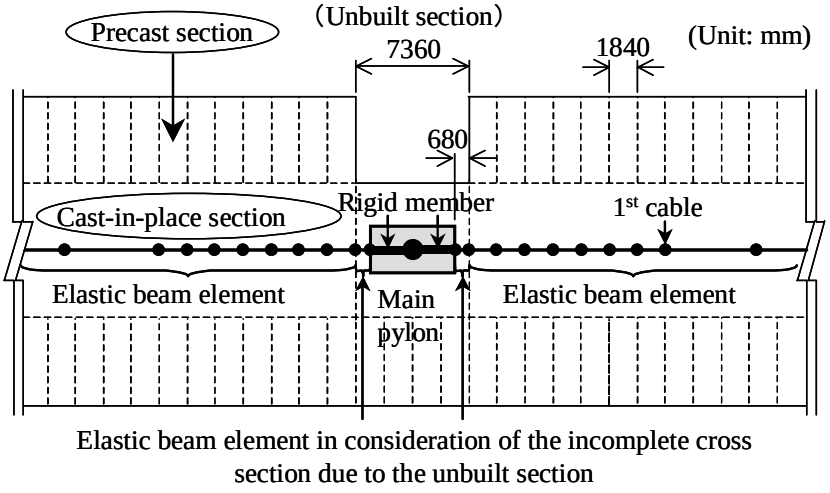

Fig. 7 Modeling of the rigid connection section of the main girder and the main pylon (Plan view)

(2) Modeling of the main pylon, pier, and foundation

The nonlinear characteristics of the bending in the elasto-plastic beam elements of the main pylon and the pier were modeled by the Takeda Model (the rigidity decrease ratio: $\gamma = 0.4$) which has a bending moment-curvature relationship of the trilinear type that takes cracking into account, in accordance with the Specifications for Highway Bridges - Seismic Design (hereafter referred to as the Bridge Specifications) [4]. As to the foundation, the collective spring constants in the horizontal, vertical, and rotating directions were calculated in accordance with the Bridge Specifications, and then a virtual rigid member was installed up to the position where the coupled term of the horizontal direction and the rotating direction becomes zero, at the bottom of which a foundation spring was installed.

3.2 Analysis Method

The axial stress acting at the bottom of the main pylon of this bridge is 7.35 N/mm^2 when the dead load is working. This is a very high axial force, about 7 times as high as that of an ordinary RC pier. Accordingly, the bending action caused by the horizontal displacement of the main pylon, the so-called P-△ effect, was taken into account in the time history response analysis. To take the geometric non-linearity into account, the local coordinate system of each member was renewed at each analysis step, and the conversion matrix between the entire coordinate system and the local coordinate system was reevaluated at each analysis step.

On the other hand, the β value (0.25) of the Newmark method was used for the numerical integration in the time history response analysis and the interval of the integration time was made to △t = 1/1000 seconds. In addition to the time-based damping of each nonlinear member, the viscosity damping constant was employed, which is 2 % for the main girder, main pylon, and pier, 20 % for the foundation, and 0% for the rigid members, and Rayleigh damping was employed for the entire system.

3.3 Input Seismic Motion

In Taiwan, a total of 631 strong motion measuring locations are being operated by the Central Weather Bureau (CWB) and many strong motion records were taken during the Chi-Chi Earthquake. The measuring location closest to the Ji-Ji-Da Bridge which could take a record during the earthquake was TCU078. It is located at 7.34 km from the bridge and 5.96 km from the hypocenter. Because the bridge is located on the same ground with TCU078 in terms of the fault as seen in Fig. 8, it is considered that the seismic motion acted on the bridge was closer to that recorded at TCU078. As the bridge lies north to south, the E-W component was installed as the perpendicular direction of the bridge and the N-S component as the axial direction, and the waveforms of the two directions were input simultaneously.

The N-S component and the E-W component of the original waveform taken at TCU078 are shown in Fig. 9 (a) and (b), respectively. The maximum acceleration at this location was 302.4 gal for the N-S component and 439.6 gal for the E-W component. From these waveforms and the direction of the fault in Fig. 8, it is known that the seismic motion of the E-W component was dominant at the bridge location. However, when these waveforms were used for analysis, the obtained results were quite different from the actual damage observed, with a small response at the main pylon and the main girder (to be explained in Section 3.4 below).

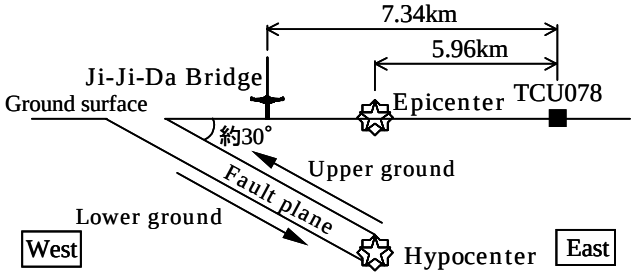

Fig. 8 Relative locations of the bridge and the strong motion measurement point (TCU078)

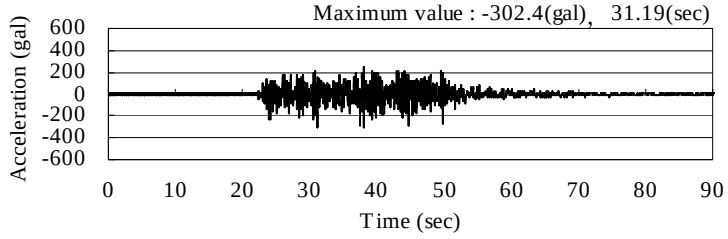

(a)TCU078（N-S）

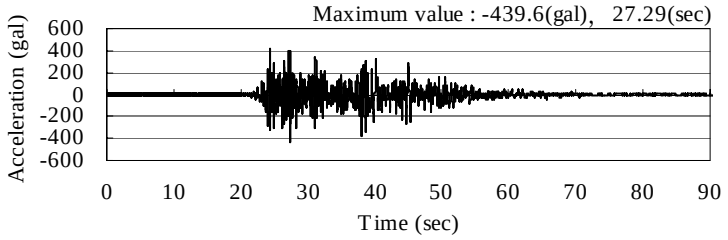

(b)TCU078（E-W）

Fig. 9 Input seismic waveform (TCU078 - original waveform)

In the meantime, according to the contour figure on the maximum acceleration in the Taichung region which was prepared by the National Center for Research in Earthquake Engineering (NCREE) in Taiwan based on a number of strong motion records during the earthquake, the estimated maximum acceleration value at the ground surface where the Ji-Ji-Da Bridge is located was 400 gal for the N-S component and 600 gal for the E-W component [5]. This means that approximately 35% larger maximum acceleration as compared with theU078 was caused in both directions.

Hence, to find an adequate input seismic motion for the current analysis, the authors paid attention to a good correlation between the H/V spectrum (the ratio of spectrums of the horizontal component and the vertical component) which was obtained through our ground micro-vibration measurements during the visit in November 2002 and the H/V of the seismic motion during the earthquake [6]. And then, the H/V spectrums at the bridge location and TCU078 were compared to estimate the seismic motion at the bridge. Figure 10 (a) shows the H/V spectrums at the bridge and TCU078. Figure 10 (b) shows the ratio of the H/V derived by dividing the H/V of the bridge by the H/V of the TCU078. With regard to the H/V of the bridge, a clear peak is seen around 0.3 seconds.

From the thickness of the surface layer at this location, 15 m, found from geological data, the velocity of shear elastic waves (Vs) is estimated to be 200 m/s and the ground type is Type II. Although a good correlation is seen between the H/V spectrums of the two locations, there is a zone where the H/V at the bridge is 1.8 times larger than that at TCU078 around a period of 2 seconds and others Hence, only the amplitude of the Fourier spectrum at TCU078 was corrected using the ratio of the H/V spectrum shown in Fig. 10 (b). And then, the waveforms of the seismic motion at the bridge was estimated using this correction, which is shown in Fig. 11. In this figure, (a) and (b) respectively show the acceleration component in the N-S and E-W directions.

The maximum acceleration at the Ji-Ji-Da Bridge which was estimated by the above process was about 50% larger in the N-S component and about 30 % larger in the E-W component as compared with those at TCU078. These are approximately equal to the maximum acceleration values estimated by the NCREE.

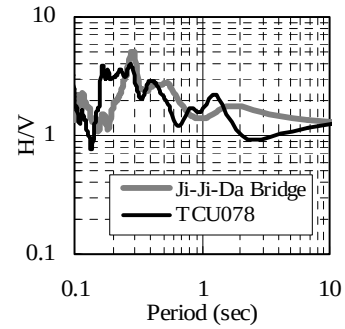

(a) H/V spectrum

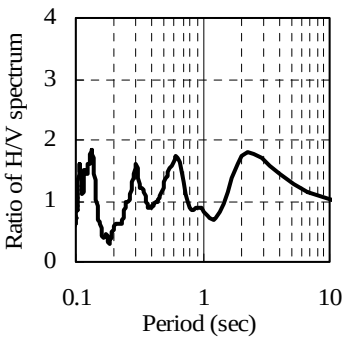

(b) H/V spectrum

Fig. 10 Measurement results of micro-vibration of the ground

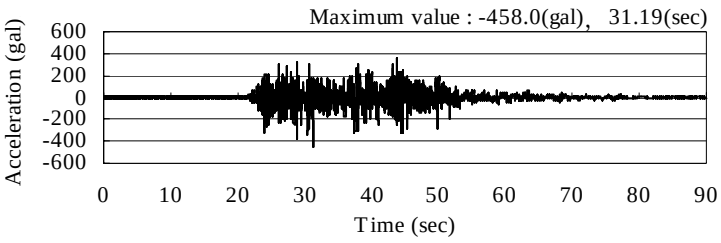

(a) TCU078 - corrected (N-S)

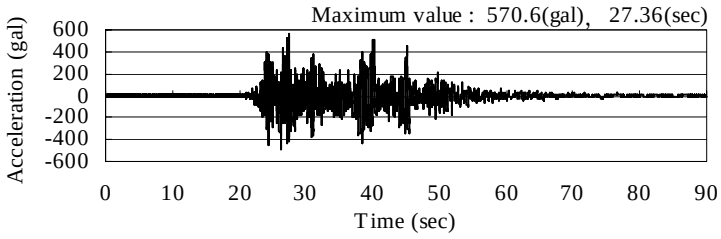

(b) TCU078 - corrected (E-W)

Fig. 11 Input seismic waveform
(TCU078 - corrected waveform)

3.4 Results of Analysis

3.4.1 Maximum response at the main girder, main pylon and pier

Figure 12 shows the response history (bending moment vs. curvature relationship) of the perpendicular direction at the bottom of the main pylon when the TCU078 original waveforms were input. According to this figure, the maximum response bending moment at the bottom of the main pylon does not reach the yield bending moment. However, according to our field observation immediately after the earthquake, the main reinforcement in the perpendicular direction buckled and the cover concrete fell at the bottom of the pylon, which is the evidence that this area reached the nonlinear range by exceeding the yield point. This means that if the TCU078 original waveforms are input, the actual damage occurred cannot be reproduced.

From the above results, it is considered that the seismic motion acted at the bridge area was probably much stronger than that given by the TCU078 original waveforms. Hence, we then used the seismic motion having approximately the same scale of maximum acceleration with that estimated by the NCREE as the input waveforms (Corrected TCU078) which are shown in Fig. 11. Figure 13 shows the response history in the axial and perpendicular directions taken at the top of the main pylon when the corrected TCU078 was input. It is seen in this figure that the maximum response displacements in the axial and perpendicular directions at the top of the main pylon are 0.14 m and 0.66 m, respectively, which means that the response in the perpendicular direction is predominant.

Table 2 shows the maximum response at the end of the main girder, the bottom of the main pylon, and the bottom of the pier where damage actually occurred during the earthquake. Shown in the table are the maximum compressive stress due to bending and the maximum compressive stress due to axial force which are obtained from the maximum

bending moment and the initial axial force. With regard to the response at the main girder, it is seen in the table that the main girder with an unbuilt section is larger in both the maximum compressive stress due to bending and the maximum compressive stress due to axial force than the main girder without an unbuilt section. The main girder without an unbuilt section here means the section on the main girder which is located next to the unbuilt section and has the largest moment among sections on the main girder because of its location closest to the main pylon. The maximum compressive stress in the axial direction of the unbuilt section of the main girder exceeds the design strength of the concrete, σck = 34.3 N/mm^2, only by the bending moment. As to the perpendicular direction, the maximum compressive stress exceeds the design strength of the concrete if the maximum compressive stress due to axial force is combined. From this, it is known that the stress acting on the cross section of the main girder of the unbuilt section is in excess of the design strength of the concrete, and that there is the possibility that a severe damage such as the fracture of concrete or the buckling of main reinforcement are caused if a seismic wave like the current case occurs.

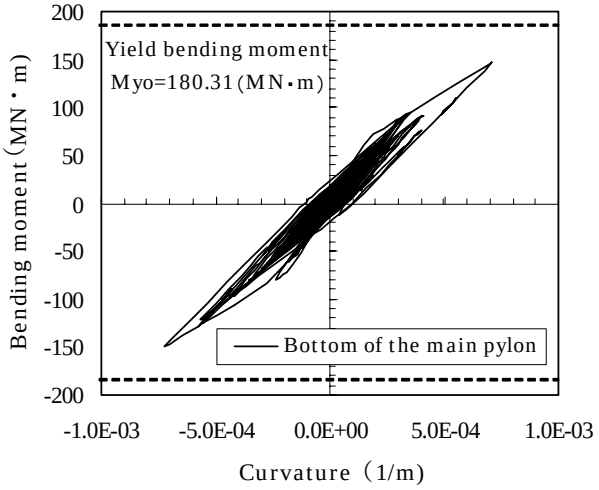

Fig. 12 Response hysteresis at the bottom of the main pylon (perpendicular direction)
(Results of the input of the TCU078 original waveform)

Table 2 Maximum response

Position	Maximum bending moment		Maximum compressive stress due to bending		Maximum curvature		Maximum axial compressive force	Maximum compressive stress due to axial force
	Axial direction	Perpendicular direction	Axial direction	Perpendicular direction	Axial direction	Perpendicular direction		
	MN・m	MN・m	N/mm^2	N/mm^2	1/m	1/m	MN	N/mm^2
Main girder (built section)	193.02	428.67	22.14	15.97	-	-	94.15	5.98
Main girder (unbuilt section)	213.30	450.08	41.65	32.11	-	-	98.04	7.80
Bottom of the main pylon	234.98	198.55	21.84	35.64	2.68E-4	2.53E-3	103.79	7.35
Bottom of the pier	512.81	472.86	26.59	23.97	1.99E-3	1.07E-3	131.48	4.37
Design strength of concrete: σck = 34.3 (N/mm^2)								

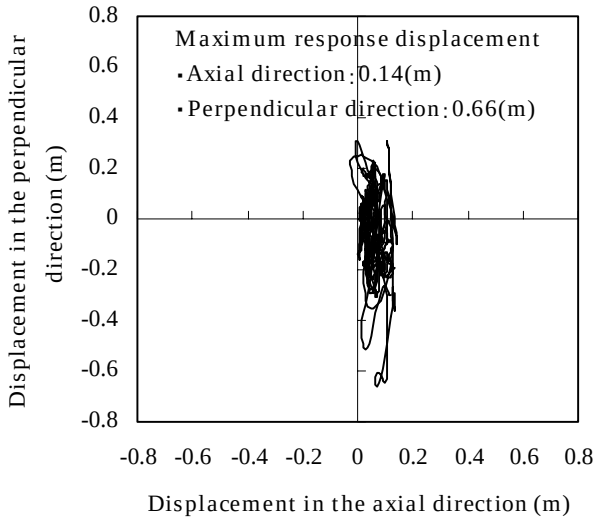

Fig. 13 Response-displacement hysteresis at the top of the main pylon

Figure 14 shows the response history (bending moment vs. curvature relationship) in the perpendicular direction at the bottom of the main pylon and the bottom of the pier. According to the analysis results, the maximum response plasticity ratio, μmax, at the pier bottom and the pylon bottom was 2.35 and 2.12, respectively, both reaching the yield strength. As to the pier bottom, this ratio is relatively in good agreement with the actual damage at the pier bottom where bending cracks occurred in the section up to 4 m from the bottom but cover concrete was not separated from the pier. As to the pylon bottom, however, the cover concrete fell from the east side face of the pylon bottom and hence it is presumed that the actual linear response was larger than the analytical results, although a relatively good agreement is seen between the analytical results and the tendency of the damage.

One of the reasons for this is the effect of the high axial force that is working on the main pylon. According to past researches on the nonlinear response of RC members having high axial force, it is known that the deformation capacity decreases because the horizontal displacement accompanies a large additional bending [7]. The axial stress working on the bottom of the pylon is 7.35 N/mm^2 under the dead load as shown in Table 2, which is approximately 7 times as high as the axial stress working on ordinary RC piers. Although the additional bending due to the horizontal displacement of the main pylon was duly considered in the analysis by the geometrical nonlinearity, a decrease in the strength due to the additional bending was not considered in the nonlinear history model of the pylon bottom, which may resulted in the underestimation of the axial stress than the actual response.

The reason that damage occurred not only at the pier bottom but also at the pylon bottom is probably due to the effect of high level modes of the main pylon. Primary modes in the perpendicular direction derived from the analysis of eigenvalues are shown in Fig. 15. In addition to the primary mode, the 5th mode and the 9th mode are predominant. As seen from the distribution of the maximum bending moment in the perpendicular direction of the main pylon and the pier shown in Fig. 16, the distribution of bending moment at the time of the maximum response at the pylon bottom differs from that at the pier bottom by the effect of high level modes.

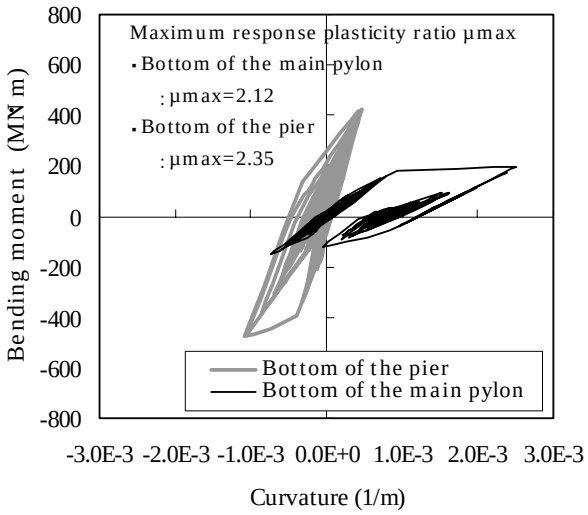

Fig. 14　Response hysteresis at the bottom of the main pylon and at the bottom of the pier

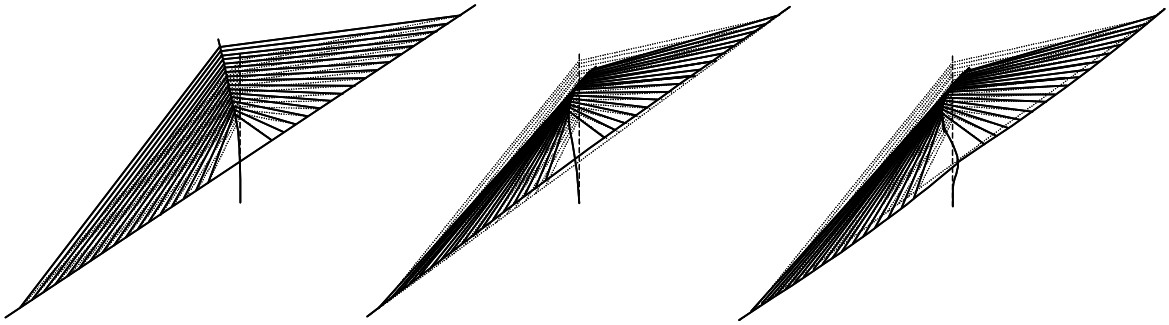

(a) The 1st mode
（T=2.080sec）

(b) The 5th mode
（T=0.637sec）

(c) The 9th mode
（T=0.230sec）

Fig. 15　Predominant mode in the direction perpendicular to the bridge axis

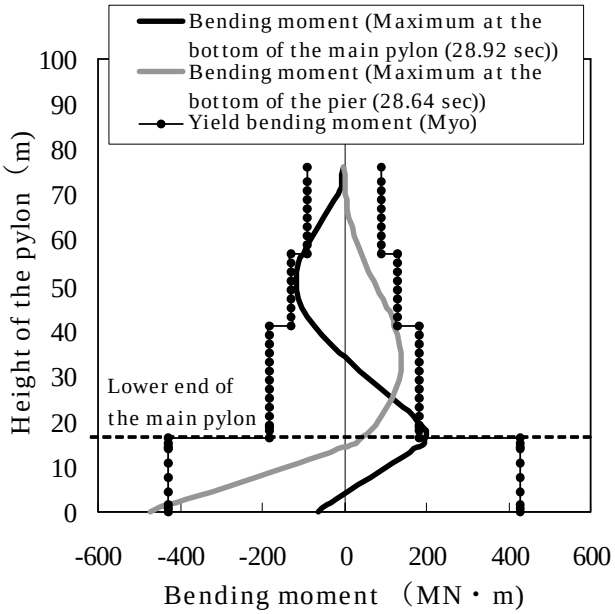

Fig. 16　Flexural strength at the main pylon and the pier and the distribution of bending moment

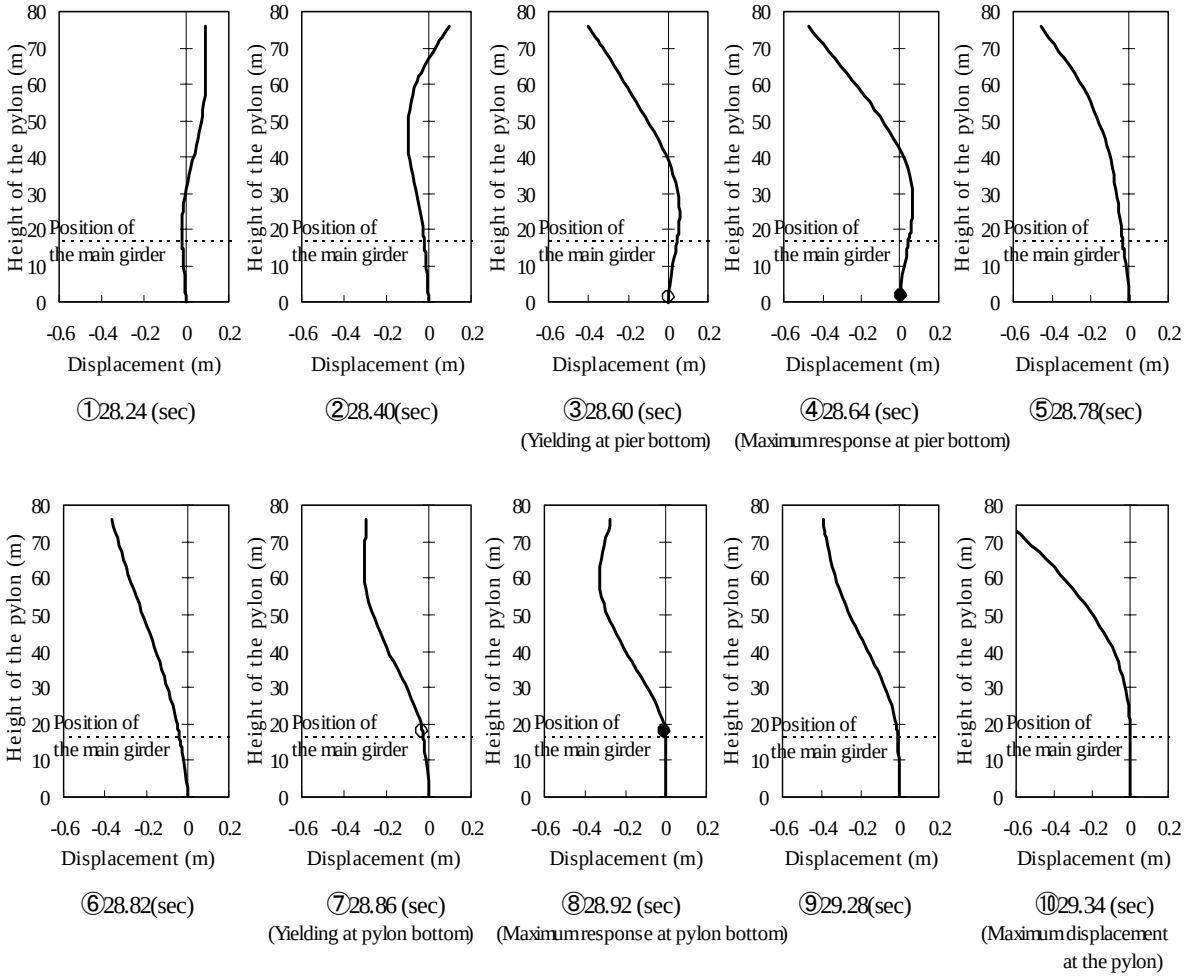

Fig. 17 Development of displacement at the main pylon and the pier

Here, to grasp the effect of the high level modes, developments of deformation at the main pylon was tracked at each time step. The deformations of the pylon seen around the time of 28.2 - 29.3 seconds which are the time of the maximum response of the pylon are shown in Fig. 17.

At ① 28.24-②28.40 seconds, the responses of the pylon bottom and the pier bottom were still elastic, but they were already showing the deformation of high level modes. At around ③28.60-④28.64 seconds, the pier bottom reached yielding by the 5th mode deformation, and immediately after that the maximum response was obtained. At this time, the pylon bottom did not yet reach yielding. At ⑤28.78-⑥28.82 seconds, the pier bottom exhibited the deformation of the primary mode in the nonlinear range. Then at ⑦ 28.86-⑧28.92 seconds, the pylon bottom reached yielding by the deformation of the 9th mode, and immediately after that the maximum response was obtained. At ⑨29.28-⑩ 29.34 seconds, both the main pylon and the pier was in the nonlinear state, at which the deformation of the primary mode was predominant and the top of the pylon reached the maximum displacement.

As seen, the pier bottom failed by the deformation of the 5th mode and the pylon bottom by that of the 9th mode, and then the nonlinear response advanced.

3.4.2 Tension force of diagonal cables

Fig. 18 shows the distribution of the maximum tension force of the diagonal cables. The initial tension, the maximum tension, and the tensile stress of the cables, numbering from 1 to 34, are shown in the figure. The difference between the maximum tension and the initial tension is the fluctuating tension associating with the seismic response. As this is a cable-stayed bridge, cables are pulled from the main pylon towards the both sides. Hence, the initial tension becomes larger as the anchorage position becomes distant from the pylon because of the effect of the cable weight and the anchoring angle. Also, as the pylon and the main girder are rigidly connected, the initial tension of cables located near the pylon is small relatively. At the time of the earthquake, construction of this bridge was almost over leaving a part of the precast section of the main girder and the deck construction. And, it is considered that an initial tension of 486 N/mm^2 on average, which is approximately 26% of the tensile strength, was introduced to the cables at the time of construction. The cross section of the cable consists of PC steel multi-strand wires having diameters of ϕ12.7 mm, 15.2 mm, and 7 mm, and the tensile strength is 1,860 N/mm^2 which is equivalent to SWPR7B.

The largest maximum stress of the cables was 720 N/mm^2 which was taken around the pullout 11th cable. But, this value is about 40% smaller compared with the design tensile strength of the cable, which is 1,860 N/mm^2. With this maximum stress value, it seems structurally impossible for the cables to be pulled out from the anchorage section.

However, when we had a talk with the bridge administrators in Taiwan in November 2002, they told us that the cable anchorage section had actually been constructed at the strength about 30% of the design tensile strength due to some construction reasons. In our analysis, the maximum tensile stress of the cables was derived as about 40% of the design tensile strength. If the actual strength of the cable anchorage was about 30% of the design tensile strength as the Taiwan administrators say, it can be said that there was the possibility that all the cables except the 14th through 21st might have been pulled out from the anchorage section. From these results, it is said that the cause of the cable pullout was the insufficient strength of cable anchorage.

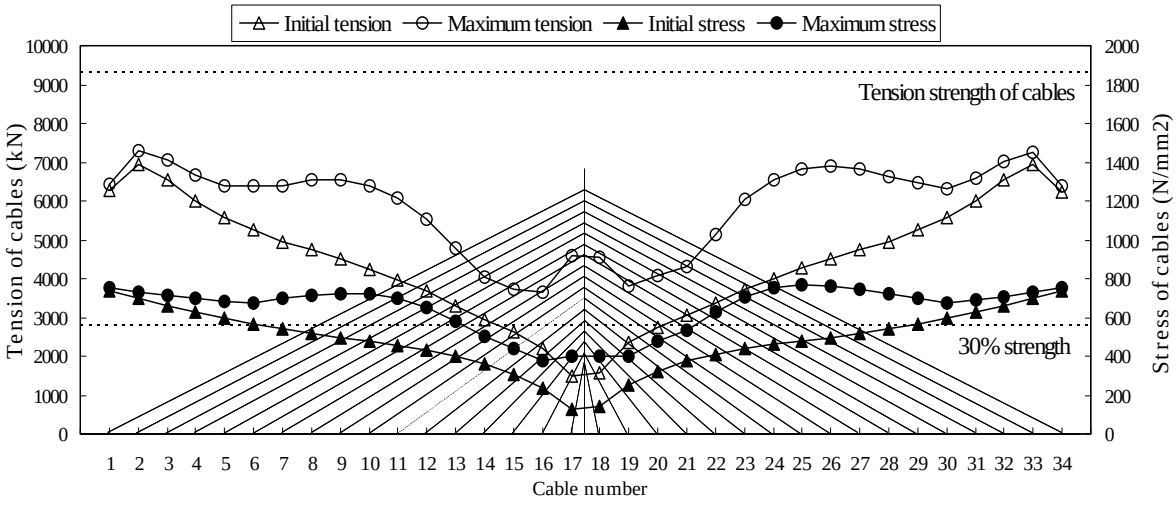

Fig. 18 Distribution of the maximum tension of the diagonal cables

4. CONCLUSIONS

The following conclusions were drawn from the seismic response analysis conducted on the cable-stayed Ji-Ji-Da Bridge damaged in the 1999 Chi-Chi Earthquake. The detailed drawings of the bridge obtained from bridge administrators in Taiwan were a great help in this analysis.

(1) The responses of the main pylon and the pier were predominant in the perpendicular direction when the seismic waves of the two directions were input simultaneously.

(2) The stress acting on the unbuilt section of the bridge was in excess of the design strength due to the bending moment and the axial force. Therefore, if a large seismic wave like that seen in the current earthquake occurs, it is possible that serious damage such as the fracture of the concrete or the buckling of the main reinforcement is caused.

(3) With regard to the cause of damage to the perpendicular direction of the main pylon, it was found from the nonlinear time history response analysis that the pier bottom reached yielding by the predominance of the 5^{th} deformation mode and the pylon bottom reached yielding by the predominance of the 9^{th} deformation mode, and then the nonlinear response advanced.

(4) It was clarified that the cause of cable pullout at this bridge was probably the insufficient anchoring strength at the time of construction.

REFERENCES

1) Kyushu Institute of Technology: *A Survey Report on Bridge Damage in the 1999 Chi-Chi Earthquake*, April 2000.

2) JSCE Working Committee on Seismic Engineering of the JSCE: *A Research Report on the Development of Seismic Design Method Based on Ultimate Bearing Capacity*, pp.567-576, March 2001.

3) Gregory L. Fenves, Charles B. Chadwell, and Stephen A. Mahin: "Near-Source Earthquake Effects on a Cable-stayed Bridge", 3^{rd} International Workshop on Performance-based Seismic Design and Retrofit of Transportation Facilities, pp.137-148, July 2002.

4) Road Association of Japan: Specifications for Highway Bridges and Commentary, V – Seismic Design, March 2002.

5) National Center for Research in Earthquake Engineering (NCREE) : *A survey Report on Bridge Damage in Sept. 21 Chi-Chi Earthquake*, NCREE-99-052, 1999.

6) Nakamura, Y. and Ueno, M.: "An Estimation of the Subsurface Ground Characteristics Utilizing Vertical Component and Horizontal Component of the Ground Surface Motion", Proceedings of the 7^{th} Earthquake Engineering Symposium of the JSCE, pp.265-270, 1986.

7) Adachi, Y., Unjoh, S., Nagaya, K., and Hayashi, M.: "Experimental Study on the Deformation Capacity of High Strength RC Members under High Axial Forces", Proceedings of the Japan Concrete Institute, Vol. 21, No. 3, 1999.